Effect of Vacuum Pretreatment on the Dyeing Properties of Wood Veneers Dyed with Camphor Fruit Pigment

Zhi Zhang,[a] Yiqing Qi, [a,]* Qiao Zu,[a] and Jianlin Han [b]

*Corresponding author: yiqingqi@njfu.edu.cn

DOI: 10.15376/biores.21.3.8303-8326

GRAPHICAL ABSTRACT

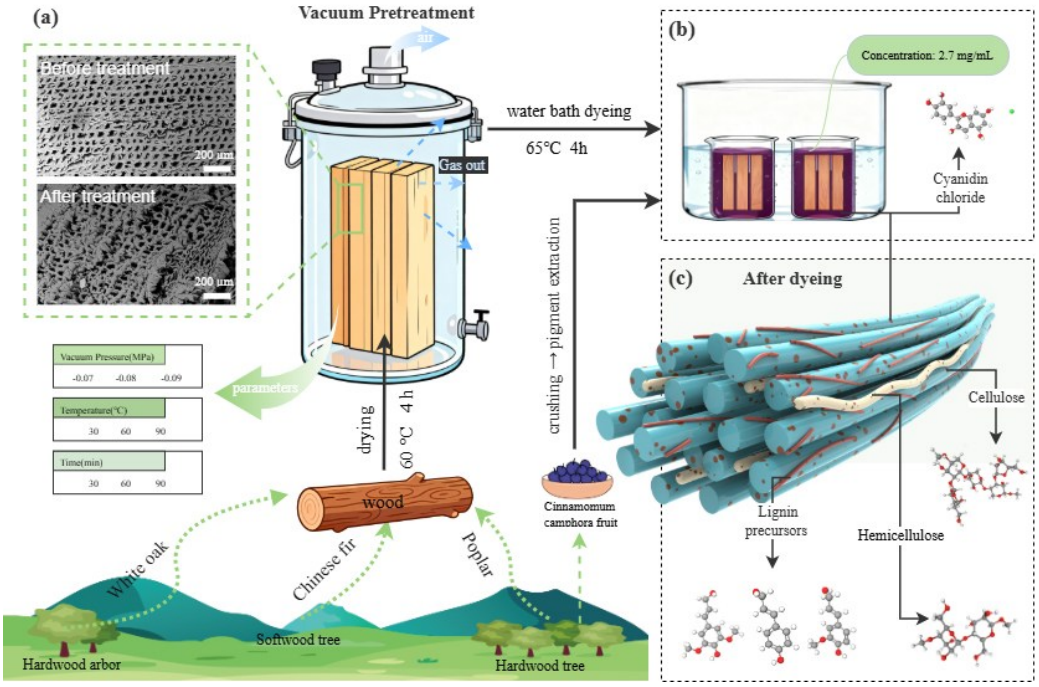

Effect of Vacuum Pretreatment on the Dyeing Properties of Wood Veneers Dyed with Camphor Fruit Pigment

Zhi Zhang,[a] Yiqing Qi, [a,]* Qiao Zu,[a] and Jianlin Han [b]

Vacuum pretreatment, valued for low energy use and sustainability, has attracted attention in wood dyeing. Using an orthogonal experimental approach, the vacuum pretreatment parameters were optimized for Chinese fir, poplar, and white oak veneers. The ideal circumstances were as follows: Chinese fir −0.08 MPa/90 °C/30 min; poplar −0.09 MPa/90 °C/30 min; and white oak −0.09 MPa/90 °C/90 min, based on color difference (Δ*E**), mass change, and water absorption weight rise. After the veneers were dyed with a camphor fruit pigment solution, the effect of the pretreatment on the microstructural alterations and macroscopic dyeing performance was assessed. The dye penetration depth and absorption rose by 60% to 95% following pretreatment. Reflectance spectra and Δ*E** values showed that the treated samples had more consistent and vibrant coloring. Additionally, there was a minor improvement in the lightfastness of all three wood types. According to microstructural research, the pretreatment increased the distribution of binding sites for interactions between dye molecules and the wood matrix by partially opening the vessel components and cell wall structures. In summary, vacuum pretreatment significantly improved the dye's homogeneity and fixing in wood veneers, offering a practical and environmentally friendly method of effective wood processing.

DOI: 10.15376/biores.21.3.8303-8326

Keywords: Vacuum pretreatment; Camphor fruit pigment dyeing; Dyeing performance; Process optimization

*Contact information: a: College of Furnishings and Industrial Design, Nanjing Forestry University, Nanjing 210037, Jiangsu, China; b: College of Chemical Engineering, Nanjing Forestry University, Nanjing 210037, Jiangsu, P. R. China; *Corresponding author: yiqingqi@njfu.edu.cn*

INTRODUCTION

Wood, an environmentally beneficial and renewable resource, is essential and irreplaceable in the construction, furniture, and decorative sectors due to its structural strength, long-term durability, and sustainability (Zhu and Niu 2022; Sun *et al.* 2024; Hassan and Grobbelaar 2025; Ljunggren *et al.* 2025). The United Nations' 2030 Agenda for Sustainable Development emphasizes the need for more sustainable management and use of forest resources (United Nations Department of Economic and Social Affairs 2021). This implies that the available supply of raw wood will be insufficient to meet future demand if management and efficiency are not improved. Therefore, improving the performance and added value of wood products is vital (Hitka *et al.* 2025). However, contemporary research mainly focuses on improving durability, fire resistance and structural stability, with less emphasis on wood pretreatment or modification prior to processing (Sandberg *et al.* 2017; Blanchet and Pepin 2021; Huang *et al.* 2024; Pang *et al.* 2025; Zhang *et al.* 2025).

Wood dyeing consists of immersing the material in a dye bath so that dye molecules penetrate the pores and adsorb onto the cell walls. However, dyeing efficiency is sometimes limited by the wood's microscopic structure, such as pore distribution and cell wall thickness, resulting in uneven coloration and reduced color fastness (Cai *et al.* 2020; Liu and Hu 2021; Shi *et al.* 2023; Qi *et al.* 2024; Zhu *et al.* 2024). Yang and Kang (2024) recognized the principal issues associated with ultraviolet light resistance and the preservation of consistent coloration during natural weathering studies on larch and fir .

Researchers have looked into several pretreatment techniques to address the aforementioned issues. For instance, alkali treatment can enlarge wood pores and enhance dye adsorption (Fang *et al.* 2023; Qi *et al.* 2023; Fang *et al.* 2025), while biological pretreatments and supercritical CO_2 pretreatment have also shown potential for improving permeability under milder or solvent-free conditions (Schwarz and Schubert 2011; Durmaz *et al.* 2016; Qi *et al*. 2025). These pretreatment techniques do have some drawbacks, though: biological pretreatment, despite being environmentally friendly, has lengthy processing cycles and challenging microbial control, which restricts its use, while alkali treatment and supercritical CO_2 pretreatment both have high energy consumption and equipment costs (Yin *et al.* 2021; Liu *et al.* 2022).

Vacuum pretreatment has attracted increasing attention as an environmentally friendly physical pretreatment strategy because it consumes less energy, leaves no chemical residues, and requires relatively simple equipment (Yang *et al.* 2021). In existing studies, vacuum treatment has most commonly been applied in the form of vacuum-assisted impregnation, in which wood is immersed in treatment solutions while vacuum is applied to remove air from the porous structure before solution penetration during pressure recovery or subsequent pressurization (Fonseca *et al.* 2023; Liu *et al.* 2023; Chen *et al.* 2021; Zhou and Liu 2022; Lemaire-Paul *et al.* 2023). For example, Fan *et al.* (2023) reported that vacuum-pressure impregnation substantially increased the bending modulus, bending strength, and dye distribution uniformity of pine veneers. However, because vacuum treatment and solution impregnation occur simultaneously in these methods, it is difficult to distinguish whether the improved dyeing performance originates from vacuum-assisted solution transport or from changes induced in the wood substrate by vacuum pretreatment itself. Consequently, studies investigating the independent effect of vacuum pretreatment prior to dyeing, particularly across different wood species, remain limited (Zhou *et al.* 2022; Chen *et al.* 2023).

The environmental friendliness of dyes is equally important in wood dyeing. Plant dyes are considered promising candidates for sustainable coloration because of their wide color range, non-toxicity, biodegradability, and abundance, and they have been widely applied in textile dyeing (Wu *et al.* 2021; Cui *et al.* 2022; Liu *et al.* 2023). The use of plant dyes in wood dyeing is still restricted, though, mainly because wood has a complicated grain structure and low permeability by nature, which results in uneven coloring and poor color fastness (Qi *et al.* 2024). Although conventional chemical pretreatments can improve dye permeability, they may damage wood structure, darken color, and increase environmental burdens due to the extensive use of chemical agents (Lu *et al.* 2023). Therefore, improving wood dyeing efficiency while maintaining ecological sustainability has emerged as a crucial area of research (Jaxel *et al.* 2020; United Nations Environment Programme 2023).

To justify the material choices in this study, three representative wood species were selected: white oak, poplar, and Chinese fir. These species differ in density, pore structure, and intrinsic permeability, which are expected to affect dye penetration, dye uptake, color uniformity, and dyeing depth. White oak, poplar, and Chinese fir, therefore, provide a suitable set of contrasting materials for evaluating wood- dyeing behavior. Camphor fruit (*Cinnamomum camphora*) was chosen as the dye source because it is locally available and contains abundant phenolic compounds and tannins, which are known to interact with wood cell wall components and mordants, making it a promising candidate for sustainable wood dyeing.

This study focused on white oak, poplar, and Chinese fir as experimental subjects. using orthogonal experiments to optimize the vacuum pretreatment parameters. Subsequently, the pretreated veneers were dyed using a natural extract from camphor fruit (*Cinnamomum camphora*). The impact of pretreatment on the microscopic structure and macroscopic dyeing performance of the three wood species is methodically examined in this work. This study advances the development of sustainable wood-processing technologies by optimizing the vacuum pretreatment procedure for these species and providing a practical, sustainable route for natural wood dyeing.

EXPERIMENTAL

Materials

The test materials were white oak (*Quercus alba* Michx.) veneer, air-dry density 0.69 g/cm³ (moisture content 12 ± 0.1%); poplar (*Populus* sp.) veneer, air-dry density 0.34 g/cm³ (moisture content 12 ± 0.1%); and Chinese fir (*Cunninghamia lanceolata*) veneer, air-dry density 0.33 g/cm³ (moisture content 12 ± 0.1%). In terms of length, width, and thickness, each veneer measured 40 mm by 40 mm by 3 mm. The camphor fruits were pitted, frozen, and ground. The ground material was mixed with deionized water whose pH had been adjusted to 1.0 using hydrochloric acid, at a solid-to-liquid ratio of 1:15 (w/v). Extraction was carried out at 60 °C with ultrasonic assistance (250 W) for 1 h. After extraction, the slurry was subjected to vacuum (suction) filtration; a layer of diatomaceous earth was spread on the filter paper prior to filtration to increase the filtration rate and to enhance the removal/adsorption of impurities from the filtrate. The resulting filtrate was used as the camphor-fruit dye extract. The tools used are listed in Table 1.

Equations

Measurement of mass change rate

Veneer specimens were weighed on an electronic analytical scale to ascertain the starting mass (M_0) following labeling and sanding with 400-mesh sandpaper. Each specimen was reweighed to determine mass M_1 once processing was finished. Equation 1 was used to determine each specimen's mass change percentage,

$$\Delta M = \frac{M_1 - M_0}{M_0} \times 100\% \quad (1)$$

where M_0 and M_1 stand for the specimen mass before and after treatment, respectively, and ΔM indicates the specimen's change of mass.

Table 1. Test Equipment

Instrument	Model	Manufacturer
Vacuum high-temperature and pressure reactor	FCF-25L	Nanjing Kair Instrument & Equipment Co., Ltd., China
Fourier transform infrared spectrometer (FTIR)	VERTEX 80V	Bruker, Germany
X-ray diffractometer (XRD)	Ultima IV	Rigaku Corporation, Japan
Scanning electron microscope (SEM)	QUANTA 200	FEI Company, USA
Colorimete	Ci6x	Shanghai Keheng Industrial Development Co., Ltd., China
UV–Vis spectrophotometer	HITACHI U-3900	Hitachi High-Tech Science Corporation, Japan
Electronic analytical balance	OHAUS	Shanghai Liangping Instrument & Meter Co., Ltd., China
Electric blast drying oven	101-3ES	Shanghai Yiheng Scientific Instrument Co., Ltd., China

Measurement of water absorption weight increase

To compare the performance before and after vacuum pretreatment, the water absorption of the wood veneers was measured using gravimetric analysis. All samples were oven-dried at 50 °C until constant mass was achieved (8 h) and then cooled to room temperature in a desiccator prior to weighing. The same drying and conditioning procedure was applied to all specimens to ensure a comparable initial moisture state before water absorption testing. The specimens were then submerged in deionized water at 25 ± 0.5 °C, and their masses were measured after 15 min, 30 min, 1 h, 2 h, 4 h, 12 h, 24 h, and 48 h of immersion. Equation 2 was used to compute the water absorption weight gain rate (*WRG*),

$$WRG\ (\%) = \frac{W_t - W_0}{W_0} \times 100 \quad (2)$$

where W_t and W_0 stand for the sample's wet and dry masses, respectively.

Chromaticity measurement

L^*, a^*, and b^* values were noted before and after pretreatment, and surface color was assessed using the CIE 1976 $L^*a^*b^*$ color space. Equation 3 was used to calculate the total color difference (ΔE^*),

$$\Delta E^* = \sqrt{(L_1^* - L_0^*)^2 + (a_1^* - a_0^*)^2 + (b_1^* - b_0^*)^2} \quad (3)$$

where ΔE denotes the total color difference; L^*_1, a^*_1, and b^*_1 are the corresponding values after treatment, while L^*_0, a^*_0, and b^*_0 are the lightness, red–green, and yellow–blue coordinates before treatment, respectively. A higher ΔE value indicates a greater overall color change (Hunter Associates Laboratory, Inc. 2008).

Determination of dye uptake

A UV-Vis spectrophotometer (HITACHI U-3900, Hitachi High-Technologies Corporation, Tokyo, Japan) was used to measure absorbance at the maximum wavelength of 514 nm. Before staining, 2 mL of dye solution was sampled, and its absorbance was recorded as A_0. Following staining, the remaining dye solution was gently mixed, brought back to 50 mL total volume, and its absorbance was recorded as A_1. Equation 4 was used to calculate dye uptake (%),

$$Ct(\%) = \frac{A_0 - A_1}{A_0} \times 100\% \quad (4)$$

where A_0 represents the absorbance of the dye solution at 514 nm before staining, in ABS, and A_1 represents the absorbance at 514 nm after staining.

Measurement of reflectance spectra and dye penetration depth

A UV-Vis spectrophotometer was used to examine the reflectance spectra of the dyed samples and assess color distribution and homogeneity. Before testing, the thickness of each dyed wood veneer (h_0) was measured at four corner positions using a digital caliper (accuracy: 0.01 mm). The corner areas were then carefully sanded with a fine woodworking rasp until the dyed layer was completely removed from the stained surface. The residual thickness (h_1) was noted, and the difference between the two was used to compute the dyeing depth (H). Each group's dyeing depth was averaged. Equation 5 was used to perform the computation,

$$H = h_0 - h_1 \quad (5)$$

where H represents the dyeing depth of the wood. h_0 and $h_1$denote the total thickness before dye removal and the residual thickness after removing the dyed layer, respectively.

Measurement of light fastness

According to ASTM G155-21, the dyed specimens' light fastness was assessed by an accelerated aging test utilizing a programmable constant temperature and humidity chamber (ASTM International 2021)(WJ-UV-150). The test parameters were 60 ± 1 °C, 50 ± 1% relative humidity, and 2 ± 0.1 W of xenon lamp output. To replicate photoaging conditions, each test cycle consisted of 40 min of water spraying after 24 h of UV irradiation.

Scanning electron microscopy (SEM) analysis

Utilizing a scanning electron microscope (QUANTA 200, FEI Company, United States), the microstructure of the wood samples was examined. Specimens were cleaned, dried, and attached to metal stubs before imaging. A small layer of gold was sputter-coated onto the surface to improve conductivity. In order to capture detailed structural details, observations were made using magnifications ranging from 600× to 20,000× and an accelerating voltage between 5 and 20 kV.

Fourier transform infrared spectroscopy (FTIR) analysis

To characterize the functional groups present in the wood veneers, Fourier transform infrared spectroscopy was performed using a VERTEX 80 spectrometer (Bruker, Germany). Prior to testing, the specimens were dried and cut into thin sections. To minimize any potential spectral interference, a single-channel background spectrum was first recorded, and 16 scans of the infrared spectra were made for each sample, ranging from 4000 to 400 cm^{-1}.

X-ray diffraction (XRD) analysis

An Ultima IV multifunctional horizontal X-ray diffractometer (Ultima Type IV, Japan, Rigaku, Tokyo, Japan) was used to analyze X-ray diffraction. Equation 6 was used to determine the cellulose's relative crystallinity index (CrL),

$$C_YL = \frac{I_{002} - I_{am}}{I_{002}} \times 100\% \quad (6)$$

where C_YL represents the relative crystallinity (%), I_{am} is the intensity of the amorphous background scattering, and I_{002} is the intensity of the diffraction peak corresponding to the (002) lattice plane (usually 20° to 22°) (Wu *et al*. 2019).

Methods

Vacuum pretreatment

All specimens were treated by sanding with 400-mesh sandpaper and drying in a forced-air oven at 60 ± 1 °C for 4 h to a target moisture content of 12.0 ± 0.1% (on a dry basis). After that, the reactor was heated to the desired temperature before the samples were placed inside. After reaching the desired level quickly, the experimenters kept the vacuum within ± 0.001 MPa and the temperature within ±2 °C. Then the vacuum was gradually released following the recommended holding time. The treated specimens were sealed and stored for later tests.

The impact of temperature, treatment time, and vacuum degree on the microscopic structure and macroscopic characteristics of wood was examined using evaluation metrics such as the mass change rate, color difference, and water absorption weight rise rate of the wood before and after treatment. Three levels are established for each factor in the pretreatment process parameters, which follow the GB/T 17657 (2022) standard. The factors and their associated levels are shown in Table 2. For each condition, four parallel samples were employed to reduce experimental error.

Table 2. Factors and Levels in the Orthogonal Test Design for Vacuum Pretreatment

Factor	Level 1	Level 2	Level 3
Vacuum level (MPa)	−0.07	−0.08	−0.09
Temperature (°C)	30	60	90
Duration (min)	30	60	90

Water bath dyeing

Chinese fir, Poplar, and white oak veneers were divided into two groups: one that received no treatment and the other that received vacuum treatment. Using white oak as an example, samples were kept in a water bath at 65 °C for 4 h (n = 4 per group) after being submerged in a camphor fruit dye solution at 2.7 mg/mL (absorbance ≈ 1.588 at λ = 514 nm). Following dyeing, the veneers were removed, any remaining surface dye was rinsed off, and the samples were oven-dried for four h at 45 ± 2 °C before being sealed for further testing.

RESULTS AND DISCUSSION

Baseline Measurement of Wood Water Absorption Capacity

To develop the ideal index of water absorption weight gain for wood and to ascertain the baseline values, the experimental process was optimized using Eq. 2. Table 3 displays the reference values for the 4 h water absorption weight gain. The 4 h water absorption percentage increases were 36.4% for Chinese fir, 36.0% for poplar, and 20.4% for white oak. The 4 h time point was selected as the reference index because it reflects the

early-stage water uptake behavior while still maintaining sufficient differentiation among different wood species. The findings show that Chinese fir and poplar exhibited higher initial water absorption performance than white oak, which was negatively correlated with the three species' variations in density (white oak 0.69 g/cm³ > poplar 0.34 g/cm³, ≈Chinese fir 0.33 g/cm³).

Table 3. Water Absorption Weight Increase Rate Reference Table

Specimen No.	poplar		Chinese fir		white oak	
1	M_0	M_1(4h)	M_0	M_1(4h)	M_0	M_1(4h)
2	2.52	3.34	1.78	2.46	3.53	4.23
3	1.64	2.27	2.13	2.69	3.06	3.73
4	1.78	2.38	2.67	3.62	3.30	4.01
5	1.72	2.34	2.08	3.04	3.78	4.36
6	1.61	2.26	2.38	3.33	3.41	4.13
7	1.60	2.18	2.10	2.79	3.39	4.07
8	1.63	2.26	2.14	2.90	3.01	3.68
9	1.78	2.39	1.95	2.67	2.85	3.50
Average	1.79	2.43	2.15	2.94	3.29	3.96
Water Absorption Rate	0.3599		0.3639		0.2043	
Percentage	35.99%		36.39%		20.43%	

Analysis of Variance and Range for Pretreatment Effects among Different Wood Species

Analysis of variance and range for white oak pretreatment

Table 4 demonstrates that temperature was the most important factor, with a range value that was noticeably greater than the vacuum degree. $A_1B_3C_2$, equivalent to a vacuum degree of −0.07 MPa, a temperature of 90 °C, and a treatment time of 60 min, was found to be the ideal procedure combination for the most significant influence on color difference. The best process combination for the most significant effect on mass change rate was $A_3B_3C_3$, corresponding to a vacuum degree of −0.09 MPa, 90 °C, and 90 min of treatment time.

Table 4. Range Analysis of Color Difference, Mass Change Rate, and Water Absorption Weight Increase Rate of Vacuum Pretreated White Oak

Indicator	Factor	K1	K2	K3	Range(R)	Priority order	Optimal combination
Color difference	Vacuum level(A)	16.515	7.549	7.549	8.966	B>A>C	$A_1B_3C_2$ (−0.07MPa, 90 °C, 60 min)
	Temperature(B)	4.255	11.171	22.240	17.985		
	Time(C)	7.433	10.687	15.602	8.169		
Weight gain rate	Vacuum level(A)	4.909	5.474	5.885	0.976	B>A>C	$A_3B_3C_3$ (−0.09MPa, 90 °C, 90 min)
	Temperature(B)	1.466	6.713	9.811	8.344		
	Time(C)	5.478	5.490	5.301	0.189		
Water absorption rate	Vacuum level(A)	1.035	1.084	1.142	0.107	B>A>C	$A_3B_3C_3$ (−0.09 MPa, 90 °C, 90 min)
	Temperature(B)	1.016	1.108	1.191	0.175		
	Time(C)	1.080	1.098	1.084	0.018		

According to the analysis of variance (Table 5), temperature significantly impacted the mass change of white oak ($p < 0.001$), and vacuum pressure also had a significant impact ($p = 0.024$). In contrast, treatment time had no statistically significant effect ($p = 0.822$). According to these findings, treatment duration had little bearing on mass change during vacuum pretreatment, while temperature and pressure were the main determinants. In the investigation of water absorption weight rise, temperature and vacuum pressure showed highly significant effects ($p < 0.001$), with a similar pattern. Additionally, treatment duration had no discernible impact ($p > 0.05$).

Table 5. Range Analysis of Color Difference, Mass Change Rate, and Water Absorption Weight Increase Rate of Vacuum Pretreated White Oak

Measure type	Source	Type III Sum of Squares	Degrees of freedom (df)	Mean square (MS)	F	Significance (p-value)
Weight gain rate	Corrected Model	26.703a	6	4.450	105.048	0.000
	Intercept	66.159	1	66.159	1561.618	0.000
	Vacuum level	0.360	2	0.180	4.245	0.024
	Temperature	26.326	2	13.163	310.701	0.000
	Time	0.017	2	0.008	0.198	0.822
	Error	1.229	29	0.042		
	Total	94.091	36			
	Corrected Total	27.931	35			
	a. $R^2 = 0.956$ (Adjusted $R^2 = 0.947$)					
Water absorption rate	Corrected Model	0.017a	6	0.003	11.587	0.000
	Intercept	2.660	1	2.660	10802.157	0.000
	Vacuum level	0.004	2	0.002	8.743	0.001
	Temperature	0.013	2	0.006	25.744	0.000
	Time	0.000	2	6.786E-05	0.276	0.761
	Error	0.007	29	0.000		
	Total	2.684	36			
	Corrected Total	0.024	35			
	a. $R^2 = 0.706$ (Adjusted $R^2 = 0.645$)					

Analysis of variance and range for poplar pretreatment

Temperature was the primary factor impacting color difference (range: 1.478), mass change (range: 7.006), and water absorption weight increase (range: 0.136), as shown in Table 6. $A_3B_3C_3$ (−0.09 MPa, 90 °C, 90 min) was the optimal combination for minimizing color difference. The ideal conditions for mass change were $A_2B_3C_1$ (−0.08 MPa, 90 °C, 30 min). The best combination for water absorption weight growth was $A_3B_3C_1$, which included a vacuum of -0.09 MPa, a temperature of 90 °C, and a treatment time of 30 min.

Temperature had a more significant impact than vacuum pressure and treatment duration on the mass change and water absorption weight rise of poplar veneers ($p < 0.001$), according to the analysis of variance in Table 7.

Table 6. Range Analysis of Color Difference, Mass Change Rate, and Water Absorption Weight Increase Rate of Vacuum Pretreated Poplar

Indicator	Factor	K1	K2	K3	Range(R)	Priority order	Optimal combination
Color difference	Vacuum level(A)	8.893	7.836	7.841	1.057	B＞C ＞A	$A_3B_3C_3$ (−0.09 MPa, 90 °C, 90 min)
	Temperature(B)	7.947	7.656	9.134	1.478		
	Time(C)	8.779	8.126	7.665	1.114		
Weight gain rate	Vacuum level(A)	5.128	5.315	4.605	0.710	B＞A ＞C	$A_2B_3C_1$ (−0.08 MPa, 90 °C, 30 min)
	Temperature(B)	1.474	6.000	8.480	7.006		
	Time(C)	5.288	5.143	4.617	0.671		
Water absorption rate	Vacuum level(A)	1.773	1.805	1.832	0.059	B＞C ＞A	$A_3B_3C_1$ (−0.09 MPa, 90 °C, 30 min)
	Temperature(B)	1.771	1.747	1.883	0.136		
	Time(C)	1.853	1.787	1.770	0.083		

Table 7. Variance Analysis of Mass Change Rate and Water Absorption Weight Increase Rate of Vacuum Pretreated Poplar

Measure type	Source	Type III Sum of Squares	Degrees of freedom (df)	Mean square (MS)	F	Significance (p-value)
Weight gain rate	Corrected Model	18.804a	6	3.134	18.185	0.000
	Intercept	56.608	1	56.608	328.473	0.000
	Vacuum level	0.203	2	0.101	0.589	0.562
	Temperature	18.414	2	9.207	53.423	0.000
	Time	0.187	2	0.094	0.543	0.587
	Error	4.998	29	0.172		
	Total	80.410	36			
	Corrected Total	23.801	35			
	a. R^2 = 0.790 (Adjusted R^2 = 0.747)					
Water absorption rate	Corrected Model	0.012a	6	0.002	0.959	0.000
	Intercept	7.315	1	7.315	3650.411	0.000
	Vacuum level	0.001	2	0.001	0.326	0.001
	Temperature	0.007	2	0.004	1.843	0.000
	Time	0.003	2	0.001	0.707	0.761
	Error	0.058	29	0.002		
	Total	7.385	36			
	Corrected Total	0.070	35			
	a. R^2 = 0.166 (Adjusted R^2 = 0.07)					

Analysis of variance and range for Chinese fir pretreatment

Table 8 indicates that temperature was the most significant element influencing the Chinese fir's performance under vacuum pretreatment. Range analysis showed that the best process combinations were (−0.07 MPa, 90 °C, 60 min), (−0.09 MPa, 90 °C, 30 min), and

(−0.08 MPa, 90 °C, 30 min) for color difference, mass change rate, and water absorption weight increase rate, respectively.

Table 8. Range Analysis of Color Difference, Mass Change Rate, and Water Absorption Weight Increase Rate of Vacuum Pretreated Chinese Fir

Indicator	Factor	K1	K2	K3	Range(R)	Priority order	Optimal combination
Color difference	Vacuum level(A)	17.457	15.512	17.032	1.945	B＞C ＞A	$A_1B_3C_2$ (−0.07 MPa, 90 °C, 60 min)
	Temperature(B)	15.226	16.746	18.374	3.148		
	Time(C)	15.567	16.330	18.105	2.539		
Weight gain rate	Vacuum level(A)	4.505	6.295	8.714	4.209	B＞A ＞C	$A_3B_3C_1$ (−0.09 MPa, 90 °C, 30 min)
	Temperature(B)	3.493	6.449	10.686	7.192		
	Time(C)	7.740	6.076	5.698	2.042		
Water absorption rate	Vacuum level(A)	2.022	2.189	2.163	0.166	B＞A ＞C	$A_2B_3C_1$ (−0.08 MPa, 90 °C, 30 min)
	Temperature(B)	1.988	2.179	2.244	0.255		
	Time(C)	2.186	2.170	2.017	0.169		

The mass change of Chinese fir veneers during vacuum pretreatment was significantly impacted by all three variables, as indicated by Table 9, where the p-values for vacuum pressure (A), temperature (B), and treatment duration (C) were all significantly below 0.001 ($p < 0.001$). (B) had a statistically significant impact on the weight increase due to water absorption ($p = 0.032$). With p-values of 0.284 and 0.117, respectively, vacuum pressure (A) and treatment duration (C) showed no significant impacts.

When combined with the range study, temperature had the most significant influence on color variation, mass change, and water absorption in all three wood species. Vacuum pressure ranked second, whereas the influence of treatment duration was relatively minor. Among the three evaluation indicators, the water absorption weight increase (WRG) was selected as the primary criterion for optimizing vacuum pretreatment because it most directly reflects the improvement in wood porosity and dye solution accessibility induced by pretreatment. Since this stage aimed to optimize the pretreatment conditions for subsequent dyeing, WRG was used as the main selection index. At the same time, color variation and mass change were retained as supplementary indicators (Tao *et al.* 2024). Accordingly, the optimal pretreatment conditions for the three wood species were Chinese fir: −0.08 MPa, 90 °C, 30 min; poplar: −0.09 MPa, 90 °C, 30 min; and white oak: −0.09 MPa, 90 °C, 90 min.P

Visual Evaluation and Color Difference Variation

Chinese fir, poplar, and white oak veneers were colored for four h at 65 °C in a water bath using a dye concentration of 2.7 mg/mL. Photographs of the samples taken before and after processing are displayed in Fig. 1. Three wood species showed varied degrees of color darkening following vacuum pretreatment, with poplar displaying the most pronounced change. In decorative wood products, color is a key aesthetic factor that influences consumer acceptance and market appeal. Therefore, the darker and more uniform appearance observed after pretreatment may improve the visual quality of the veneers and enhance their potential value in furniture and interior decoration applications.

Table 9. Variance Analysis of Mass Change Rate and Water Absorption Weight Increase Rate of Vacuum Pretreated Chinese Fir

Measure type	Source	Type III Sum of Squares	Degrees of freedom (df)	Mean square (MS)	F	Significance (p-value)
Weight gain rate	Corrected Model	29.400a	6	4.900	42.389	0.000
	Intercept	95.202	1	95.202	823.558	0.000
	Vacuum level	6.697	2	3.348	28.966	0.000
	Temperature	20.934	2	10.467	90.544	0.000
	Time	1.770	2	0.885	7.656	0.002
	Error	3.352	29	0.116		
	Total	127.955	36			
	Corrected Total	32.753	35			
	a. R^2 = 0.898 (Adjusted R^2 = 0.876)					
Water absorption rate	Corrected Model	0.050a	6	0.008	2.799	0.028
	Intercept	10.154	1	10.154	3423.860	0.000
	Vacuum level	0.012	2	0.006	2.028	0.150
	Temperature	0.025	2	0.012	4.153	0.026
	Time	0.013	2	0.007	2.216	0.127
	Error	0.086	29	0.003		
	Total	10.290	36			
	Corrected Total	0.136	35			
	a. R^2 = 0.367 (Adjusted R^2 = 0.236)					

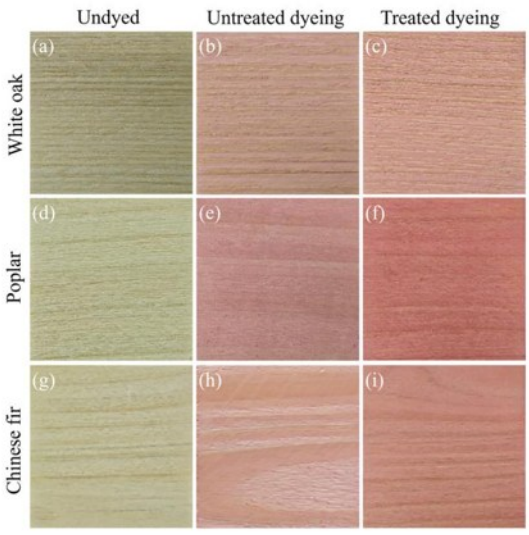

Fig. 1. Visual appearance of camphor fruit dye on three wood species

Table 10. The Color Difference (Δ*E*) Values of Chinese Fir, Poplar, and White Oak Before and After Vacuum Pretreatment

Wood group	Undyed			Dyed			Color difference (Δ*E**)				
	L^*_0	a^*_0	b^*_0	L^*_1	a^*_1	b^*_1	Δ*L**	Δ*a**	Δ*b**	Δ*E**	Average ΔE*
Untreated White oak	71.33	7.62	20.93	61.83	21.66	16.83	−9.50	14.04	−4.10	17.45	16.31
	67.94	8.51	21.83	60.28	21.18	17.97	−7.66	12.67	−3.86	15.31	
	67.76	8.59	21.44	59.40	22.16	17.50	−8.36	13.57	−3.94	16.44	
	66.71	8.56	21.11	58.41	21.76	17.36	−8.30	13.20	−3.75	16.05	
Pretreated White oak	73.58	6.3	19.54	62.35	22.1	15.32	−11.23	15.79	−4.22	19.84	18.97
	73.86	6.43	20.07	62.75	22.26	15.71	−11.11	15.83	−4.36	19.84	
	73.77	6.44	19.77	62.91	22.05	15.37	−10.86	15.61	−4.4	19.53	
	70.85	7.64	21.39	64.64	22.1	17.46	−6.21	14.45	−3.93	16.67	
Untreated Poplar	76.62	5.29	18.20	64.44	21.56	15.06	−12.18	16.27	−3.14	20.57	20.44
	74.44	5.92	18.32	63.44	22.20	15.47	−10.99	16.28	−2.85	19.86	
	73.90	6.02	18.30	62.81	22.40	15.75	−11.09	16.38	−2.55	19.95	
	77.48	5.93	18.40	64.47	22.48	14.72	−13.01	16.55	−3.67	21.38	
Pretreated Poplar	75.46	6.48	18.82	62.83	23.53	15.59	−12.63	17.06	−3.23	21.48	23.32
	75.66	6.33	18.92	62.38	23.89	15.55	−13.28	17.56	−3.37	22.27	
	75.67	6.32	18.77	60.72	25.62	15.66	−14.95	19.30	−3.11	24.62	
	77.67	5.62	17.84	62.03	24.75	14.79	−15.64	19.13	−3.05	24.91	
Untreated Chinese fir	70.20	9.26	23.16	60.46	18.13	17.75	−9.74	8.87	−5.41	14.29	18.24
	71.20	7.84	21.70	58.91	19.59	15.64	−12.29	11.75	−6.06	18.06	
	74.79	7.15	22.55	60.76	22.11	17.61	−14.03	14.96	−4.94	21.10	
	71.36	7.77	20.95	58.19	20.70	14.66	−13.17	12.93	−6.29	19.52	
Pretreated Chinese fir	71.52	8.58	22.52	55.13	22.77	17.31	−16.39	14.19	−5.21	22.32	24.47
	76.91	5.90	20.77	58.49	23.30	17.33	−18.42	17.41	−3.44	25.58	
	74.43	6.97	21.25	55.61	23.64	16.58	−18.83	16.67	−4.67	25.58	
	73.11	7.65	21.92	55.56	23.57	16.27	−17.55	15.93	−5.65	24.41	

The color difference (ΔE) values of Chinese fir, poplar, and white oak before and after vacuum pretreatment are shown in Table 10. The ΔE value is a popular statistic for assessing dyeing success, where greater values denote more noticeable color changes. In general, vacuum-treated samples had greater ΔE values than untreated ones. In particular, there was a 13.7% increase in the poplar's ΔE value, from 20.4 to 23.3. The ΔE increased from 16.3 to 19.0 (16.2%) for white oak and 18.2 to 24.5 (34.0%) for Chinese fir, which showed the most significant rise. According to these findings, vacuum pretreatment improved the dyeing performances of several wood species to varying degrees, with Chinese fir and poplar showing the greatest gains.

Analysis of Dye Penetration Depth in Wood Veneers

White oak, poplar, and Chinese fir veneers stained with camphor fruit pigment are shown in Fig. 2 along with the dyeing depths of the untreated and vacuum-pretreated veneers. Three species showed a discernible improvement in dyeing depth after processing. The average dyeing depth rose from 0.90 mm (untreated) to 1.42 mm (pretreated) for Chinese fir and from 1.12 to 1.82 mm for white oak. The average depth of poplar increased from 1.42 to 2.48 mm, the most noticeable improvement among the three. Inherent anatomical characteristics of poplar may be responsible for this notable improvement. As a species that grows quickly, poplar has a loosely structured, porous structure, thinner fiber cell walls than Chinese fir, and increased permeability as a result. Camphor fruit pigment, an acidic natural color, has an excellent affinity for poplar and forms ionic connections with the acetyl groups (-$COCH_3$) of hemicellulose (Wang *et al.* 2017; Penttilä *et al.* 2021).

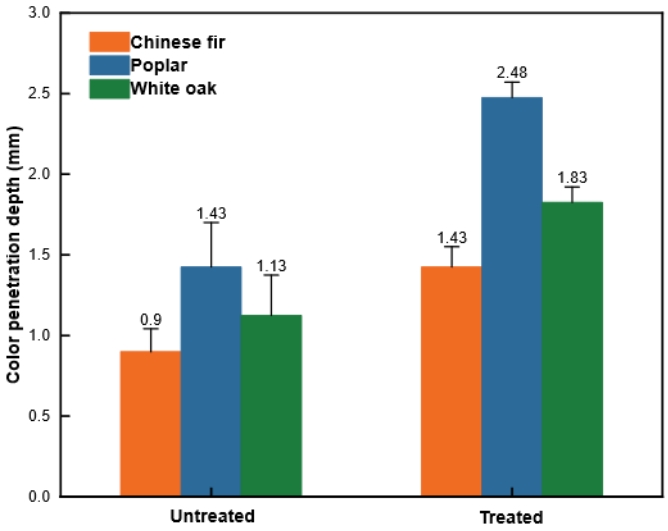

Fig. 2. Comparison of the dyeing depth of wood veneers dyed with camphor fruit pigment

Dye Uptake Rate

As shown in Fig. 3, untreated Chinese fir, poplar, and white oak exhibited relatively low dye uptake percentages of 7.4%, 7.9%, and 5.4%, respectively, after immersion dyeing. The inherent anatomical structure and limited permeability of wood restrict the penetration and distribution of dye molecules during immersion dyeing, resulting in relatively low dye uptake and poor color uniformity (Dorvel *et al.* 2018; Widsten *et al.* 2022). All three wood species showed significant increases in dye uptake following vacuum pretreatment: Chinese fir rose to 14.4%, poplar rose to 13.1%, and white oak rose

to 8.6%. Vacuum pretreatment may have improved the accessibility of the wood structure to the dye solution during the subsequent immersion process, thereby facilitating dye penetration into vessels, tracheids, and intercellular spaces. This contributes to a more uniform distribution of dye within the wood structure and improves the overall dyeing performance. Poplar and Chinese fir exhibited the most improvement out of the three, suggesting that their loosely packed and more porous cellular structures react more favorably to the increased permeability brought on by vacuum treatment. White oak also exhibited improved dye uptake, although the increase was comparatively smaller, which may be attributed to its denser anatomical structure.

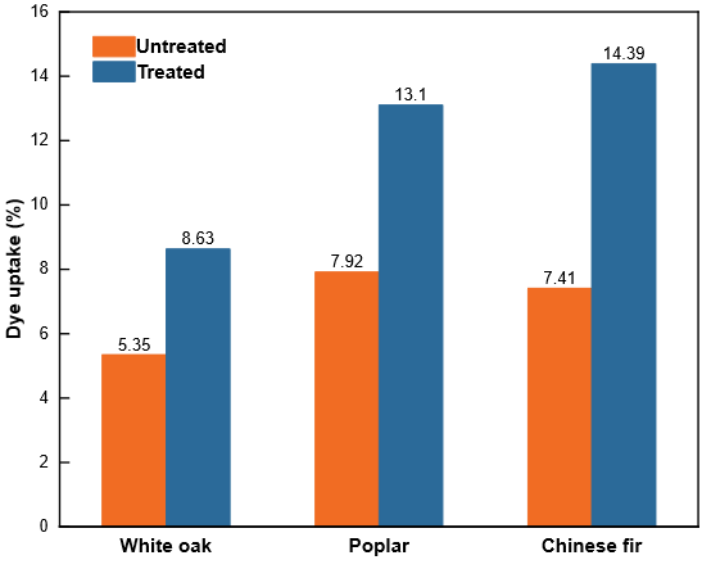

Fig. 3. Dye uptake of the three wood species before and after pretreatment

Scanning Electron Microscopy (SEM) Analysis of Microstructure

SEM images of untreated white oak, vacuum-treated white oak, and vacuum-treated white oak following dyeing are shown in Fig. 4. The untreated specimen (Fig. 4a) exhibited visible extractive deposits within the vessel lumens. Following vacuum pretreatment (Fig. 4b), fewer visible extractive deposits were observed within the lumens, and pit apertures were more clearly visible in the representative field of view. After dyeing (Fig. 4c), dye deposits were observed on the cell walls and within the vessel lumens. These observations are qualitatively consistent with the improved dye accessibility after vacuum pretreatment

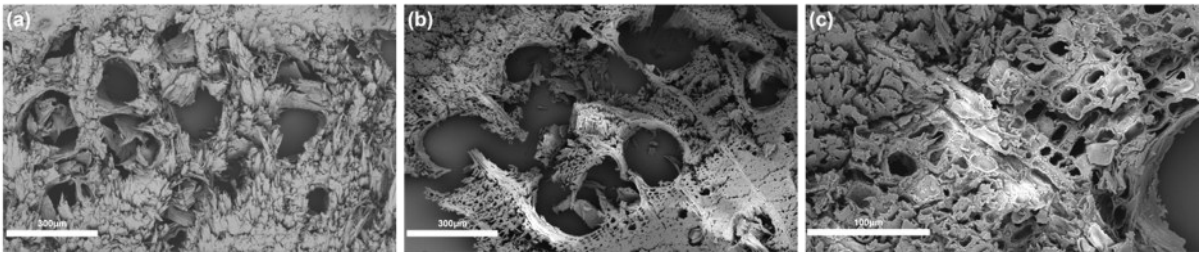

Fig. 4. (a) Untreated white oak (400×); (b) Vacuum-treated white oak (400×); (c) Vacuum-treated and dyed white oak (1600×).

Poplar's microstructural characteristics are shown in Fig. 5 before and after vacuum pretreatment and dyeing. The untreated specimen (Fig. 5a) exhibited extractive deposits on the inner vessel surfaces. Following vacuum pretreatment (Fig. 5b), fewer visible extractive deposits and clearer pit apertures were observed in the representative field of view. Dye deposits were observed on the cell walls and within the vessel lumens after dyeing (Fig. 5c), consistent with the improved dye uptake measured for the vacuum-pretreated specimens.

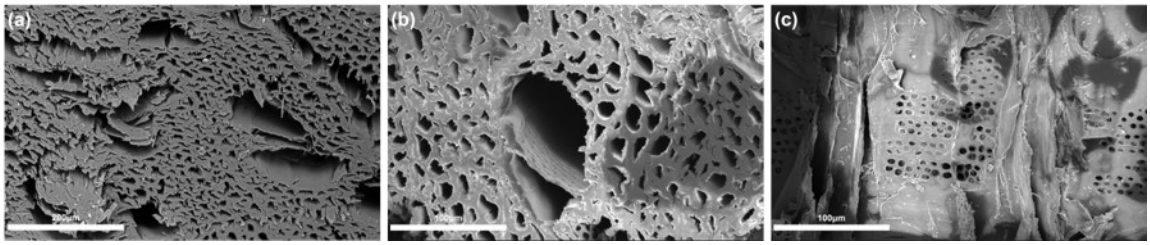

Fig. 5. (a) Untreated poplar (800×); (b) Vacuum-treated Poplar (1600×); (c) Vacuum-treated and dyed poplar (1600×).

Figure 6 presents SEM images of Chinese fir before and after vacuum pretreatment and subsequent dyeing. Compared with the untreated specimen (Fig. 6a), the vacuum-pretreated specimen (Fig. 6b) exhibited fewer visible deposits within the tracheid lumens, and bordered pit apertures were more clearly visible in the representative field of view. Dye deposits were observed on the tracheid walls and within the lumens after dyeing (Fig. 6c). These observations qualitatively support the macroscopic dyeing results.

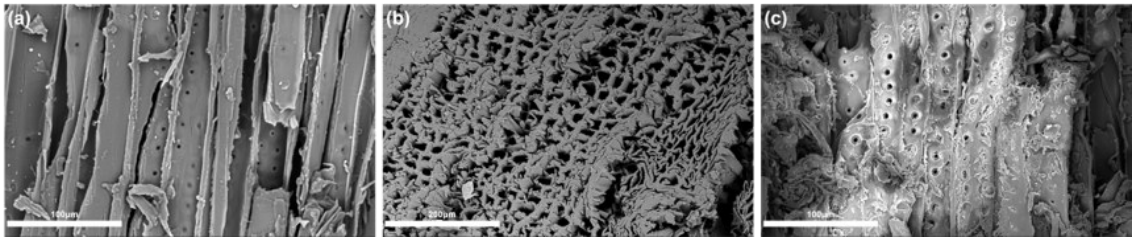

Fig. 6. (a) Untreated Chinese fir (1600×); (b) Vacuum-treated Chinese fir (800×); (c) Vacuum-treated and dyed Chinese fir (1600×).

Fourier Transform Infrared (FTIR) Spectroscopy Analysis

Figure 7 shows the FTIR spectra of untreated, untreated-dyed, and vacuum-pretreated-dyed specimens of Chinese fir, poplar, and white oak. The spectra were compared to evaluate differences in characteristic absorption bands among the three sample groups. No new characteristic absorption bands or obvious shifts in peak positions were observed after vacuum pretreatment, although differences in the relative intensities of several existing bands were detected. Compared with the untreated wood, the dyed specimens exhibited increased absorbance at approximately 1735 cm^{-1} and 1592 cm^{-1} for all three wood species. These increases are more likely attributable to the presence of dye components containing carbonyl- and aromatic functional groups. The corresponding absorption bands of these dye components may overlap with those of wood. Therefore, the observed increases are unlikely to indicate chemical changes in the wood cell-wall components. Compared with the dyed specimens without vacuum pretreatment, vacuum-pretreated white oak exhibited relatively higher absorbance at 3334 cm^{-1} and 1243 cm^{-1}.

Similarly, poplar showed relatively stronger absorbance at 3342 cm^{-1} and 1726 cm^{-1} after vacuum pretreatment (Liu *et al.* 2023; Cheng *et al.* 2025), while Chinese fir exhibited relatively higher absorbance at 1593 cm^{-1} and 1028 cm^{-1}. Overall, vacuum pretreatment did not substantially alter the chemical structure of the wood cell-wall components. Instead, the observed differences in band intensity are more likely attributable to differences in the amount and distribution of dye components retained within the wood following vacuum pretreatment.

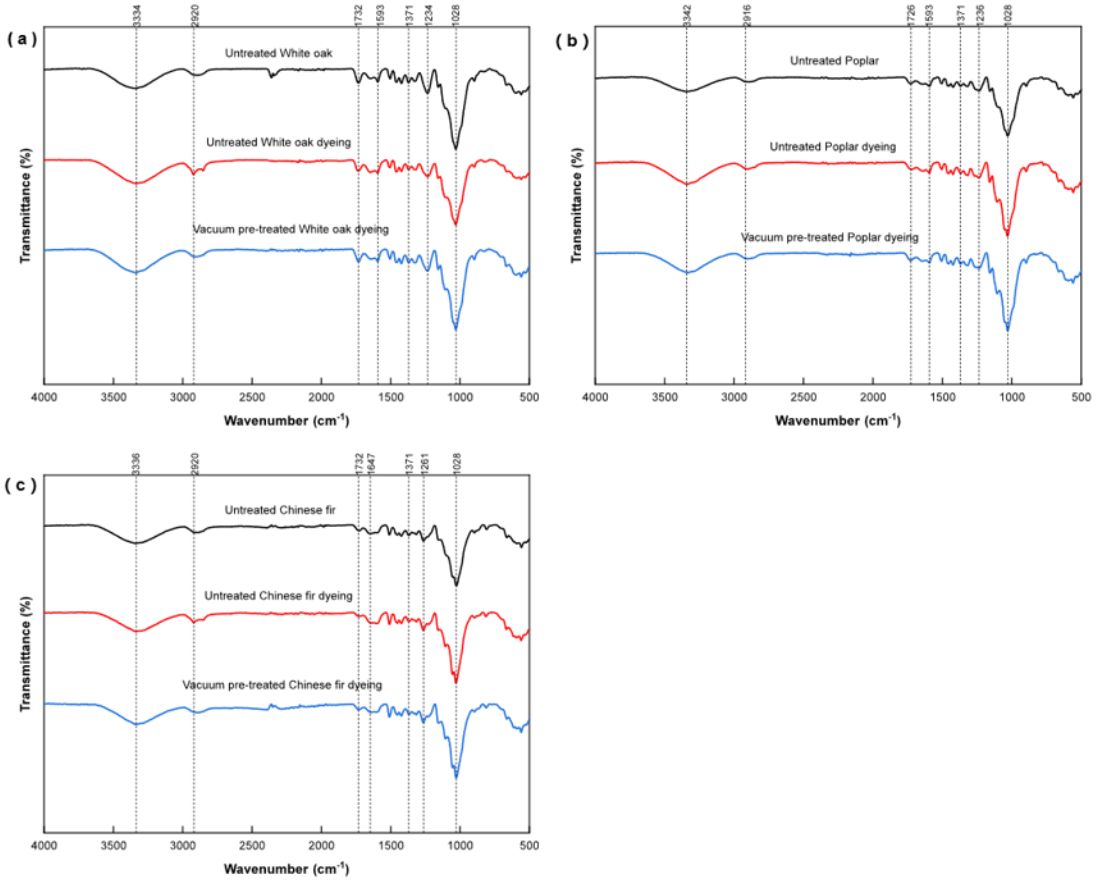

Fig. 7. FTIR spectra of white oak, Poplar, and Chinese fir before treatment, after conventional dyeing, and after vacuum pretreatment followed by dyeing with camphor fruit pigment

X-ray Diffraction (XRD) Analysis

The X-ray diffraction (XRD) patterns of the three wood species after dyeing with and without vacuum pretreatment are shown in Fig. 8. Characteristic diffraction peaks were observed at 2θ values of approximately 18°, 22°, and 34°, corresponding to the (101), (002), and (040) crystallographic planes, respectively. The vacuum-pretreated specimens showed no discernible changes in diffraction peak positions or overall diffraction patterns compared with the dyed specimens without vacuum pretreatment, suggesting that vacuum pretreatment had little influence on the crystalline structure of cellulose. The calculated crystallinity values of the three wood species are summarized in Table 11. Although differences were observed in the calculated crystallinity values after vacuum pretreatment (Table 11), no obvious changes in diffraction peak positions or overall diffraction patterns were detected. Therefore, these differences are unlikely to represent substantial changes in the crystalline structure of cellulose under the mild treatment conditions used in this study. Overall, the XRD results indicate that vacuum pretreatment did not substantially alter the

crystalline structure of the three wood species. Accordingly, the improved dyeing performance observed after vacuum pretreatment is unlikely to be associated with changes in cellulose crystallinity.

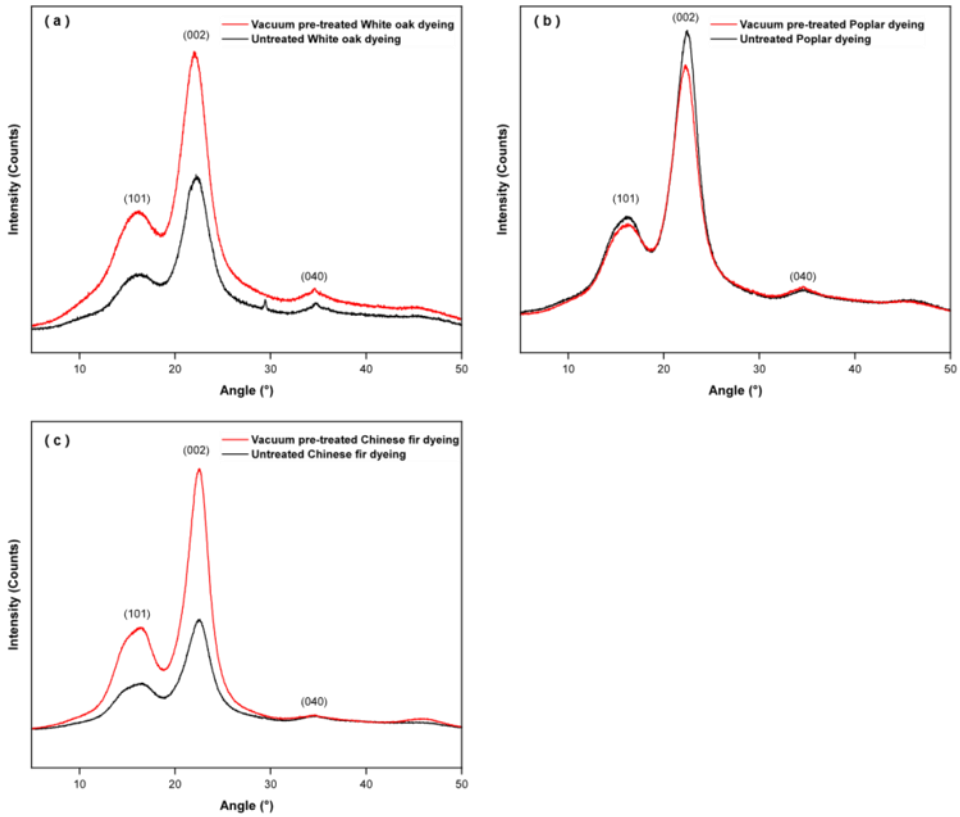

Fig. 8. XRD patterns of (a) white oak, (b) poplar, and (c) Chinese fir before treatment and after vacuum pretreatment followed by dyeing

Table 11. Calculated Crystallinity Values of the Dyed Veneers Before and After Vacuum Pretreatment

Wood species	Dyed without vacuum pretreatment (%)	Vacuum-pretreated and dyed (%)
White oak	76.7	61.6
Poplar	72.9	69.2
Chinese fir	64.8	74.1

Reflectance Spectrum Analysis of Dyed Veneers

The reflectance spectra of Chinese fir, poplar, and white oak dyed with *Cinnamomum camphora* fruit pigment were obtained in this work by averaging the reflectance data of each sample before and after vacuum pretreatment, as illustrated in Fig. 9. The same trends seen in the reflectance curves of the three wood types indicate a uniformity in coloration following dyeing. All three dyed wood species had slightly lower reflectance in the 400 to 500 nm wavelength range than their untreated counterparts. This suggests that the flavonoids in the camphor fruit pigment had a weaker absorption of blue-violet light (around 450 nm), which comparatively enhances the violet component in the reflectance spectrum. The reflectance in the 450 to 600 nm region exhibited a downward-

then-upward "V"-shaped trough and was dramatically lowered compared to the untreated samples, demonstrating increased absorption of yellow light and decreased brightness following dyeing. This behavior is consistent with lignin-dye compounds' distinctive absorption of mid-wavelength light (Zhu *et al*. 2018). Interestingly, the reflectance spectra of Chinese fir that have been treated and untreated were nearly identical. This is explained by the inherent structural properties of Chinese fir, which indicate that deeper-layer measurements are required for a more accurate assessment because light absorption and reflection on the surface after dyeing remain largely consistent. However, compared to the dyed, untreated samples, the reflectance of the dyed, pretreatment samples for poplar and white oak was notably higher. This suggests that the wood's surface microstructure is altered by vacuum pretreatment, leading to more consistent light absorption and reflection following dyeing.

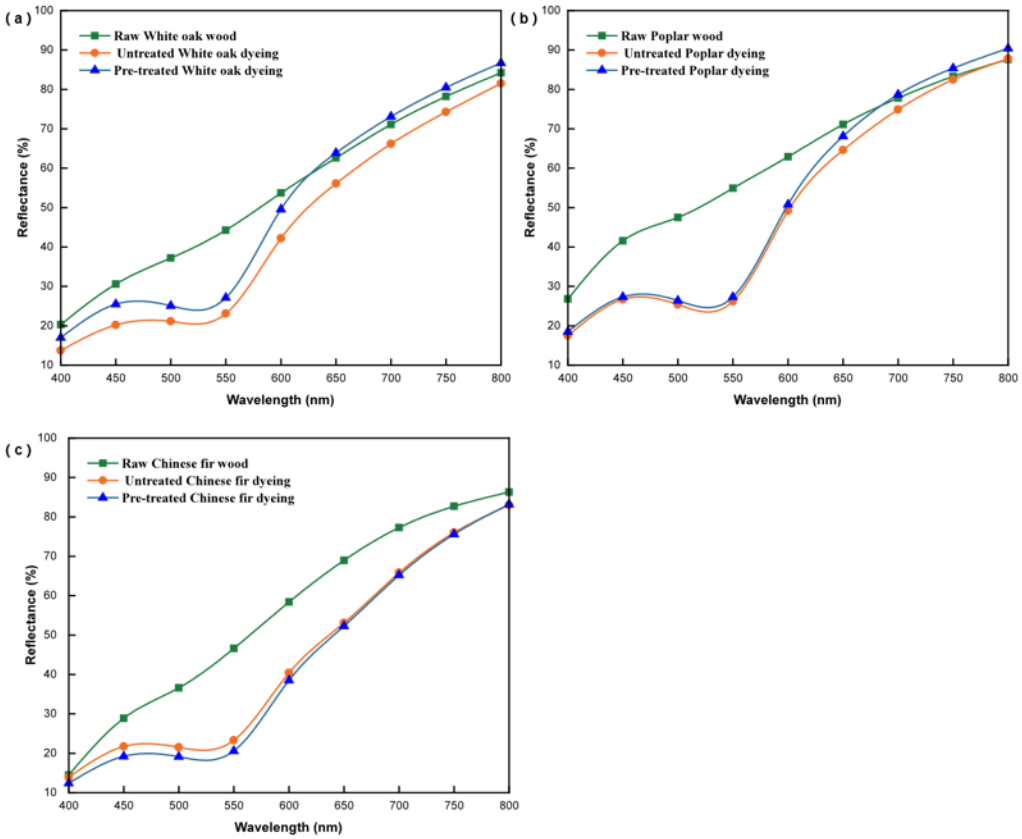

Fig. 9. Reflectance spectra of three wood species dyed with *Cinnamomum camphora* fruit pigment before and after vacuum pretreatment: (a) white oak, (b) poplar, (c) Chinese fir

Lightfastness Analysis of Dyed Veneers

The lightfastness of the three wood veneers dyed after vacuum pretreatment was evaluated by a sunlight exposure test. The color difference after light exposure between the pretreated and untreated samples was calculated according to Eq. 2, as illustrated in Fig. 10. Lightfastness was assessed using color difference; a lower ΔE^* indicates greater lightfastness. All three species' ΔE^* values dropped during vacuum pretreatment, suggesting differing levels of lightfastness improvement. However, this does not mean that the color change was permanent; rather, it indicates improved color stability under accelerated aging conditions. Poplar exhibited the most noticeable decline of all of them,

with ΔE^* dropping from 6.51 to 6.12. These outcomes align with the microstructural descriptions: SEM showed that the pretreated group had fewer free-surface pigments and deeper, more consistent pigment penetration. Cellulose crystallinity remained steady, according to XRD. These results imply that vacuum pretreatment increases the lightfastness of the dyed samples by encouraging deeper pigment fixing and lowering fading-prone surface components.

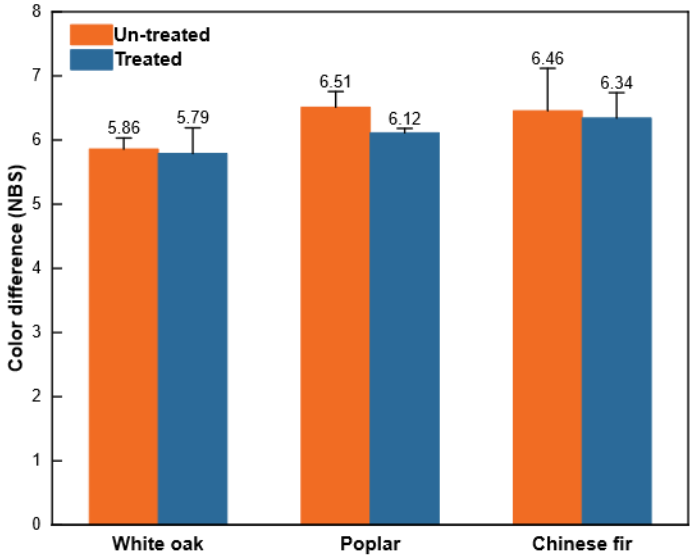

Fig. 10. Light-induced color difference (ΔE^*) of three dyed wood veneers before and after pretreatment after sunlight exposure.

CONCLUSIONS

1. The range and variance studies' results showed that temperature, followed by vacuum degree, was the main factor influencing color difference, mass change, and water absorption weight rise. Treatment duration, however, showed a negligible impact. The following were the ideal vacuum pretreatment parameters for the three wood species, based on their overall water absorption performance: −0.09 MPa, 90 °C, 90 min for white oak; −0.09 MPa, 90 °C, 30 min for poplar; and −0.08 MPa, 90 °C, 30 min for Chinese fir.
2. The macroscopic dyeing performance was greatly enhanced by vacuum pretreatment. The dye uptake rate rose from 5.4% to 8.6% for white oak (+61.3%), from 7.9% to 13.1% for poplar (+65.4%), and from 7.4% to 14.4% for Chinese fir (+94.2%) as compared to the untreated group. In the meantime, dyeing depth and post-dyeing color difference (ΔE) both increased to differing degrees; for instance, ΔE for Chinese fir climbed from 18.2 to 24.5 and for colored poplar, from 20.4 to 23.3, suggesting that pretreatment increases color uniformity and dye absorption.
3. Scanning electron microscope (SEM) observations did not reveal substantial anatomical changes, while Fourier transform infrared (FTIR) and X-ray diffraction (XRD) analyses indicated no detectable alterations in the chemical composition or crystalline structure of the wood following vacuum pretreatment. Therefore, the improved dyeing performance observed after vacuum pretreatment is unlikely to be

attributable to detectable anatomical, chemical, or crystalline structural changes in the wood under the mild treatment conditions used in this study.

4. In accelerated aging tests, the sunlight-induced color difference (ΔE) of all three species decreased to varying degrees: Poplar ΔE decreased from 6.5 to 6.1, (white oak) ΔE decreased from 5.9 to 5.8, and (Chinese fir) ΔE decreased from 6.5 to 6.3. Overall, lightfastness under sunlight exposure was improved, which correlated with the observed microscopic changes. This suggests that the pretreatment improved photostability by encouraging deeper fixation of pigments and lowering the quantity of free pigments at the surface.

ACKNOWLEDGMENTS

Conflict of Interest

The authors declare that they have no known competing financial interests or personal relationships that could have appeared to influence the work reported in this paper.

REFERENCES CITED

ASTM International. (2021). "Standard practice for operating xenon-arc lamp apparatus for exposure of materials," ASTM International, West Conshohocken, PA.

Blanchet, P., and Pepin, S. (2021). "Trends in chemical wood surface improvements and modifications: A review of the last five years," *Coatings* 11, article 1514. https://doi.org/10.3390/coatings11121514

Cai, C. Y., Zhou, F. D., and Cai, J. B. (2020). "Bound water content and pore size distribution of thermally modified wood studied by NMR," *Forests* 11(12), article 1358. https://doi.org/10.3390/f11121358

Chen, K., Zhu, J., Tan, Y., Sun, F., Gan, J., Peng, H., Zhan, T., and Lyu, J. (2023). "Development of gradient-wetting Janus wood membrane with high-efficiency fog collection and oil-water separation," *Chemical Engineering Journal* 470, article 144356. https://doi.org/10.1016/j.cej.2023.144356

Chen, Z. R., Zhang, S., Ding, M., Wang, M., and Xu, X. (2021). "Construction of a phytic acid–silica system in wood for highly efficient flame retardancy and smoke suppression," *Materials* 14(15), article 4164. https://doi.org/10.3390/ma14154164

Cheng, P., Zhong, T., Long, J., Li, J., Shi, J., Xu, C., and Chen, H. (2025). "Green manufacturing of bamboo self-bonding composites with superior mechanical and electromagnetic interference shielding performance," *Eur. J. Wood Prod.* 83, article 163. https://doi.org/10.1007/s00107-025-02317-w

Cui, H. Y., Xie, W., Hua, Z., Cao, L., Xiong, Z., Tang, Y., and Yuan, Z. (2022). "Recent advancements in natural plant colorants used for hair dye applications: A review," *Molecules* 27(22), article 8062. https://doi.org/10.3390/molecules27228062

Dorvel, B., Boopalachandran, P., Chen, I., Bowling, A., Williams, K., and King, S. (2018). "Probing the effect of polymer molecular weight on penetration into the wood cell wall using polyethylenimine (PEI) as a model compound," *J. Microsc.* 270(2), 121-128. https://doi.org/10.1111/jmi.12663

Durmaz, S., Hafizoğlu, H., and Tümen, I. (2016). "Investigation of enzymatic effects on

pit membranes using light and scanning electron microscopy," *Drewno* 59(198), 163-169. https://doi.org/10.12841/wood.1644-3985.107.12

Fan, S. T., Gao, X., Pang, J., Liu, G., and Li, X. (2023). "Enhanced preservative performance of pine wood through nano-xylan treatment assisted by high-temperature steam and vacuum impregnation," *Materials* 16(11), article 13976. https://doi.org/10.3390/ma16113976

Fang, X. Y., Li, H., Zhang, Y., Chen, C., and Wang, X. (2023). "The effect of alkali treatment on the crystallinity, thermal stability, and surface roughness of bamboo fibers," *Fibers and Polymers* 24(2), 505-514. https://doi.org/10.1007/s12221-023-00059-5

Fang, X. Y., Li, H., Zhang, Y., Chen, C., and Wang, X. (2025). "The effect of alkali treatment on the mechanical strength, thermal stability, and water absorption of bamboo fiber/PLA composites," *Forests* 16(1), article 64. https://doi.org/10.3390/f16010064

Fonseca, L., Silva, H., and Abrantes, I. (2023). "Industrial assays to evaluate the efficacy of vacuum pressure impregnation with commercial wood preservatives to eliminate the pinewood nematode, *Bursaphelenchus xylophilus*, and other nematodes from *Pinus pinaster* wood," *European Journal of Wood and Wood Products* 81(5), 1147-1159. https://doi.org/10.1007/s00107-023-01943-6

GB/T 17657-2022 (2022). "Test methods for physicochemical properties of engineered wood-based panels and surface-finished panels," Standardization Administration of China (SAC), Beijing.

Hassan, F. S., and Grobbelaar, S. (2025). "Assessing the feasibility of structural timber construction in South Africa," *Wood Materials Science & Engineering*. (in press).

Hitka, M., Joščák, P., Sedliačik, J., and Kminiak, R. (2025). "Improving joint strength through controlled wood swelling," *Wood Material Science & Engineering*. https://doi.org/10.1080/17480272.2025.2466844

Huang, Y., Zheng, Z., Chen, C., Guo, C., Wang, X., Zhou, Q., and Tu, D. (2024). "Effective strategy for fabricating surface impregnated and unilaterally densified wood with furfuryl alcohol/flame retardants for enhanced mechanical performance and flame retardancy," *European Journal of Wood and Wood Products* 82(3), 731-745. https://doi.org/10.1007/s00107-023-02043-1

Hunter Associates Laboratory, Inc. (2008). CIE Lab color scale*. Technical Report. Reston, VA, USA.

Jaxel, J., Gusenbauer, C., Böhmdorfer, S., Liebner, F., and Hansmann, C. (2020). "Improving single-step $scCO_2$ dyeing of wood by DMSO-induced micro-swelling," *Journal of Supercritical Fluids* 165, article 104978. https://doi.org/10.1016/j.supflu.2020.104978

Lemaire-Paul, M., Beuthe, C. A., Riahinezhad, M., and Foruzanmehr, M. R. (2023). "The impact of vacuum pressure on the effectiveness of SiO_2 impregnation of spruce wood," *Wood Science and Technology* 57(1), 147-171. https://doi.org/10.1007/s00226-022-01448-0

Liu, H. H., Xie, J. G., and Zhang, J. W. (2022). "Moisture transfer and drying stress of *Eucalyptus* wood during supercritical CO_2 ($ScCO_2$) dewatering and $ScCO_2$ combined oven drying," *BioResources* 17(3), 5116-5128. https://doi.org/10.15376/biores.17.3.5116-5128

Liu, H., Zhang, Y., *et al.* (2023). "Advancements in sustainable natural dyes for textile applications: A review," *Molecules* 28(16), article 155954.

https://doi.org/10.3390/molecules28165954
Liu, H., Zhou, T., Sun, X., and Zong, G. (2023). "Organosilane-modified wood materials: A review of research and applications," *Bioresources* 18(3), 6561-6582. https://doi.org/10.15376/biores.18.3.liu
Liu, J. M., Kong, X., Wang, C., and Yang, X. (2023). "Permeability of wood impregnated with polyethylene wax emulsion in vacuum," *Polymer* 281, article 126123. https://doi.org/10.1016/j.polymer.2023.126123
Liu, Y., and Hu, J. (2021). "Investigation of polystyrene-based microspheres from different copolymers and their structural color coatings on wood surface," *Coatings* 11(1), article 24. https://doi.org/10.3390/coatings11010024
Ljunggren, F., Fredriksson, M., Johansson, N., and Sasic Kalagasidis, A. (2025). "Cross-laminated timber: A state-of-the-art review of moisture, fire, acoustics, and energy-related aspects," *Wood Materials Science & Engineering*, 1-23. https://doi.org/10.1080/17480272.2025.2507145
Lu, D., Xiong, X., Lu, G., Gui, C., and Pang, X. (2023). "Effects of $NaOH/H_2O_2/Na_2SiO_3$ bleaching pretreatment method on wood dyeing properties," *Coatings* 13(2), article 233. https://doi.org/10.3390/coatings13020233
Pang, Y., Sun, J., Xu, J., Zhang, W., Zhou, J., Liu, Y., Guo, H., and Jiang, F. (2025). "Hierarchical supramolecular engineering of a multifunctional phase-change material with thermally switchable properties for adaptive thermal management," *Advanced Functional Materials* 2024, article 16260. https://doi.org/10.1002/adfm.202416260
Penttilä, P. A., Zitting, A., Lourençon, T., Altgen, M., Schweins, R., and Rautkari, L. (2021). "Water-accessibility of interfibrillar spaces in spruce wood cell walls," *Cellulose* 28(18), 11231-11245. https://doi.org/10.1007/s10570-021-04253-3
Programme, United Nations Environment Programme (UNEP). (2023). Specialized Manual on Green and Sustainable Chemistry Education and Learning. United Nations Environment Programme. https://doi.org/10.59117/20.500.11822/44540
Qi, Y. Q., Sheng, Y. T., Liu, G. Y., Han, J. L., and Shen, L. M.. (2025). "Effect of supercritical carbon-dioxide pretreatment on the permeability and plant dyeing performance of three wood species," *Wood Material Science & Engineering* 2025, article 2519556. https://doi.org/10.1080/17480272.2025.2519556
Qi, Y. Q., Zhang, Y., Liu, Y., Wang, X., and Zhou, Q. (2023). "Effect of NaOH pretreatment on permeability and surface properties of three wood species," *ACS Omega* 8(43), 40362-40374. https://doi.org/10.1021/acsomega.3c04841
Qi, Y. Q., Zhang, Y., Liu, Y., Wang, X., and Zhou, Q. (2024). "Study on the dyeing properties of Chinese fir with Cinnamomum camphor pigment by premordant dyeing," *Wood Material Science & Engineering* 20(1), 166-176. https://doi.org/10.1080/17480272.2024.2335672
Qi, Y. Q., Zhang, Z., Sun, Y., Shen, L., and Han, J. (2024). "Study on the process optimization of peanut coat pigment staining of poplar wood," *Forests* 15(3), article 504. https://doi.org/10.3390/f15030504
Sandberg, D., Kutnar, A., and Mantanis, G. (2017). "Wood modification technologies – A review," iForest - Biogeosciences and Forestry 10(6), 895-908. https://doi.org/10.3832/ifor2380-010
Schwarz, F. W. M. R., and Schubert, M. (2011). "*Physisporinus vitreus*: a versatile white rot fungus for engineering value-added wood products," *Applied Microbiology and Biotechnology* 92(3), 431-440. https://doi.org/10.1007/s00253-011-3539-1
Shi, H., Chen, Y., Zhang, Y., Wang, X., and Zhou, Q. (2023). "Chemical structure and

microscopic morphology changes of dyed wood holocellulose exposed to UV irradiation," *Polymers* 15(5), article 1186. https://doi.org/10.3390/polym15051186

Sun, J. M., Xu, J. N., Zhou, S. J., Pang, Y., Zhang, W. Y., Zhou, J., Liu, Y., Guo, H. W., and Jiang, F. (2024). "Enhancing building energy efficiency: Leaf transpiration inspired construction of lignin-based wood plastic composites for building energy conservation," *Applied Energy* 367, article 123448. https://doi.org/10.1016/j.apenergy.2024.123448

Tao, M., Liu, X., and Xu, W. (2024). "Effect of the vacuum impregnation process on water absorption and nail-holding power of silica sol-modified Chinese fir," *Forests* 15(2), article 270. https://doi.org/10.3390/f15020270

United Nations Department of Economic and Social Affairs. (2021). "Global Forest Goal 4," in: The Global Forest Goals Report 2021, United Nations, New York, NY. (https://www.un.org/esa/forests/wp-content/uploads/2021/04/Global-Forest-Goals-Report-2021).

Wang, X. Q., Wang, F., Yu, Z., Zhang, Y., Qi, C., and Du, L. (2017). "Surface free energy and dynamic wettability of wood simultaneously treated with acidic dye and flame retardant," *Journal of Wood Science* 63(3), 271-280. https://doi.org/10.1007/s10086-017-1621-8

Widsten, P., Chittenden, C., West, M., Thumm, A., and Donaldson, L. (2022). "Enzymatic treatments for improved dyeing of solid wood," *Holzforschung* 76, 493-502. https://doi.org/10.1515/hf-2021-0230

Wu, Y., X. Wu, T. Shi, H. Chen, H. Wang, M. Sun, and J. Zhang (2019). "The microstructure and mechanical properties of poplar catkin fibers evaluated by atomic force microscope (AFM) and nanoindentation," *Forests* 10(11), article 938. https://doi.org/10.3390/f10110938

Wu, Y., Zhou, J., Yang, F., Wang, Y., Wang, J., and Zhang, J. (2021). "A strong multilayered transparent wood with natural wood color and texture," *Journal of Materials Science* 56(13), 8000-8013. https://doi.org/10.1007/s10853-021-05833-1

Yang, H., Gao, M., Wang, J., Mu, H., and Qi, D. (2021). "Fast preparation of high-performance wood materials assisted by ultrasonic and vacuum impregnation," *Forests* 12(5), article 567. https://doi.org/10.3390/F12050567

Yang, S. M., and Kang, S. G. (2024). "Assessment of color and contact angle changes in waterborne stained wood under natural weathering condition of South Korea's summer climate," *BioResources* 19(1), 1666-1679. https://doi.org/10.15376/biores.19.1.1666-1679

Yin, X. Y., Wei, L. S., Pan, X. Y., Liu, C., Jiang, J., and Wang, K. (2021). "The pretreatment of lignocelluloses with green solvent as biorefinery preprocess: A minor review," *Frontiers in Plant Science* 12, article 670061. https://doi.org/10.3389/fpls.2021.670061

Zhang, S., Wang, M., Huang, Y., Zhang, Y., and Yu, W. (2025). "Effects of iron oxide-modified hierarchically porous 4A zeolites on flame retardancy of ammonium polyphosphate-treated wood composites," *RSC Advances* 15(28), 22565-22575. https://doi.org/10.1039/D5RA03148F

Zhou, J., Wang, Y., Wang, J., and Wu, Y. (2022). "Multilayer transparent wood with log color composed of different tree species," *ACS Omega* 7, 46303-46310. https://doi.org/10.1021/acsomega.2c04842

Zhou, T., and Liu, H. H. (2022). "Research progress of wood cell wall modification and functional improvement: A review," *Materials* 15(4), 1504-1598.

https://doi.org/10.3390/ma15041598
Zhu, J. G., and Niu, J. Y. (2022). "Green material characteristics applied to office desk furniture," *BioResources* 17(2), 2228-2242. https://doi.org/10.15376/biores.17.2.2228-2242
Zhu, T., Liu, S., Ren, K., Chen, J., Lin, J., and Li, J. (2018). "Colorability of dyed wood veneer using natural dye extracted from different organic solvents," *BioResources* 13(4), 7197-7211. https://doi.org/10.15376/biores.13.4.7197-7211
Zhu, Z. P., Li, Y., Liu, Y., Wang, X., and Jiang, Z. (2024). "Effect of unilateral surface compression technique and heat treatment on industrial application performance of poplar," *Industrial Crops and Products* 211, article 117004. https://doi.org/10.1016/j.indcrop.2024.117004

Article submitted: March 8, 2026; Peer review completed: June 12, 2026; Revised version received: June 24, 2026; Further revised version received and accepted: June 28, 2026; Published: July 16, 2026.
DOI: 10.15376/biores.21.3.8303-8326